RSC Advances

PAPER

View Article Online
View Journal | View Issue

Cite this: *RSC Adv.*, 2020, **10**, 6584

The characterization and evaluation of the synthesis of large-ring cyclodextrins (CD_9–CD_{22}) and α-tocopherol with enhanced thermal stability

Chuan Cao,[ab] Li Xu,[a] Peng Xie,[c] Jinwei Hu,[a] Jun Qi,[a] Yibin Zhou*[a] and Lei Cao[d]

Received 20th December 2019
Accepted 21st January 2020

DOI: 10.1039/c9ra10748g

rsc.li/rsc-advances

Large-ring cyclodextrins LR-CDs (CD_9–CD_{22}) were obtained from rice starch using cyclodextrin glycosyltransferase (CGTase), and were used as a wall material for embedding α-tocopherol. Complexes of α-tocopherol and LR-CDs were prepared by co-precipitation. A molar ratio of α-tocopherol/LR-CD of 1 : 2 showed the highest encapsulation efficiency. The surface morphology of the complex particles was observed to vary from irregular flakes to the formation of smaller clusters of particles using scanning electron microscopy (SEM). Based on ^{1}H NMR and FT-IR observations, the inclusion complexes exhibited significant chemical shifts of 0.3 ppm and decreased peak signals. In addition, thermal analysis showed that the microcapsules improved the thermostability of the α-tocopherols. Antioxidant activity analysis proved the stability of α-tocopherol during storage. This study could serve as a reference for the more effective use of LR-CDs as wall materials.

1. Introduction

Macrocyclodextrin is a cyclodextrin in which the cyclic glucose units have a degree of polymerization of more than nine through 1,4 glycosidic bonds. The structure of macrocyclodextrin is different from the hollow barrel structure of common small cyclodextrins owing to the large degree of polymerization.[1,2] The structure of macrocyclodextrin has been reported, and it is similar to a hollow structure, with a hydrophobic cavity.[3] When the degree of polymerization is less than 14, it has a large hydrophobic inner cavity. When the degree of polymerization is 26, it folds into an "8" shape with two hydrophobic cavities.[4,5] The aqueous solubility of LR-CDs is greater than that of β-CD, it is biologically similar to starch, and it is safe and non-toxic. Meanwhile, the structure of the LR-CDs also reveals unique embedding properties,[6] which make it a good wall material. However, less research has been conducted on macrocyclodextrins specifically for the encapsulation of compounds. The synthesis of LR-CDs from tapioca starch was evaluated by Kuttiyawong *et al.* (2015), who optimized the synthesis reaction and the characterization of the large-ring cyclodextrin (LR-CD) products, however, no further comparisons of the inclusion complexes, physical mixing, and free forms were studied.[7]

Studies on improving the adverse properties of tocopherol, including complexes of β-cyclodextrin or its derivatives,[8] the nano-encapsulation of osa-starch[9] and the formation of liposomes[10] have been reported. However, the embedding of macrocyclodextrin and tocopherol has not been studied until now. The changes in the structure during the formation of the complex can lead to different physicochemical properties. Therefore, research into the changes in the structural and physicochemical properties of the LR-CDs–α-tocopherol inclusion complexes is necessary.

The present study reveals the synthesis of LR-CDs (CD_9–CD_{22}) obtained from rice starch by combining CGTase with pullulanase. We formed a complex between the LR-CDs and α-tocopherol using the co-precipitation method and characterized its macrocyclodextrin inclusion complex. The complexation of macrocyclodextrin protects the guest substance. This research could serve as a reference for the more effective use of macrocyclodextrin as a wall material, accounting for its solubility and low viscosity, thus expanding the application of LR-CDs in food, medicine, and other fields.

2. Experimental

2.1 Materials

The LR-CDs standards with degrees of polymerization from CD_{22}–CD_{50} were purchased from Ezaki Glico Co., Ltd. (Japan). Cyclodextrin glucanotransferase (CGTase, EC 2.4.1.19) was obtained from Amano Enzyme Co., Ltd. (Japan). Pullulanase (1498 NPUN/g) and α-tocopherol were provided by Sigma Aldrich (Chemical Co. St. Louis, MO, USA). Rice starch was obtained from Guangming Huaixiang biotechnology (Hefei, China).

[a]*Anhui Engineering Laboratory for Agro-products Processing, Anhui Agricultural University, Hefei 230036, China. E-mail: zhouyibin@ahau.edu.cn*
[b]*Anhui Vocational College of Grain Engineering, Hefei 230011, China*
[c]*Nanjing University of Finance and Economics, China*
[d]*Institute of Agro-Products Processing, Anhui Academy of Agricultural Sciences, China*

2.2 Synthesis of LR-CDs

Rice starch (5% w/v) and acetic acid buffer (0.01 M, pH 5.5) were added into a 500 mL Erlenmeyer flask, boiled and stirred for 30 min followed by cooling to 55 °C. Then, pullulanase (100 U g^{-1}) was added, followed by further incubation for 12 h at 55 °C and at pH 5.5. The reaction was stopped by boiling for 10 min. The above mixture was cooled to 60 °C, then CGTase (8 U g^{-1}) was added followed by further incubation for 2 h at 60 °C and pH 5.5. The reaction products were determined using a previously reported method.[12] Subsequently, ethanol precipitation was carried out for 12 h at ambient temperature followed by centrifugation at 5000 rpm for 10 min (JW-1016; Jiaven Equipment Industry Co., Ltd., Jiangsu, P. R. China). After centrifugation, the sediments were washed with anhydrous ethanol and vacuum dried (DGT-G-C; Darth carter Experimental Instrument Co., Ltd., Shanghai, P. R. China) at 40 °C to obtain the LR-CDs.

2.3 Characterization of the LR-CD product

The matrix assisted laser ionization-time of flight-mass spectrometry (MALDI-TOF-MS) (New ultrafleXtreme, Bruker Daltonics Inc) spectra were determined using a previously reported method.[13]

2.4 Preparation of the inclusion complexes

The α-tocopherol/LR-CDs inclusion complexes were prepared using the previously reported method[14] with some modifications. LR-CDs (2 g) and distilled water were added into a 20 mL Erlenmeyer flask at 55 °C and stirred for 30 min. Followed by cooling to ambient temperature, α-tocopherol was added to the obtained different molar fractions of the α-tocopherol complexes. The LR-CDs and α-tocopherol were mixed in a molar ratio of 1 : 1, 1 : 1.5, 1 : 2, 1 : 2.5, 1 : 3. Then, the mixtures were protected from exposure to direct light and stirred for 4 h at 30 °C. Subsequently, the optimization of the co-precipitation in aqueous solution was performed using ultrasound for 60 min, and later it was maintained overnight at 4 °C to achieve a balanced reaction. The precipitated α-tocopherol/LR-CDs clathrate was recovered by vacuum drying to obtain the embedded product.

2.5 Preparation of the α-tocopherol and LR-CD physical mixture

The physical mixture of α-tocopherol and LR-CD was prepared at a molar ratio of 1 : 2 at the same ratio of α-tocopherol in the inclusion complex. LR-CDs were ground into a mortar with α-tocopherol and the ingredients were mixed with a spatula to obtain a homogeneous mixture.

2.6 Encapsulation efficiency

Quantitation of α-tocopherol was performed using a spectrophotometer at 292 nm (UV-vis Spectrophotometer, Beijing Purkinje general instrument).[15] The content of α-tocopherol formed in the complexes was calculated based on the previously described procedure.[16] The LR-CDs–α-tocopherol complexes were dissolved in 95% ethanol for 24 h followed by centrifugation at 4000 rpm for 10 min (JW-1016; Jiaven Equipment Industry Co., Ltd., Jiangsu, P. R. China). After centrifugation, the supernatant was retained. The standard curve regression equation for the ethanol solution of α-tocopherol was $A = 0.00651C - 0.01016$, $R^2 = 0.9995$ zz at 292 nm.

In which A is the absorbance and C is the mass concentration (μg mL^{-1}).

The encapsulation efficiency (EE) was calculated according to the following formulas.[17]

$$EE = \frac{\text{Amount of entrapped active compound}}{\text{Initial amount of active compound}} \times 100 \quad (1)$$

2.7 Analysis of LR-CD–α-tocopherol complexes

2.7.1 Scanning electron microscopy. The morphology of the starch granules was determined using Hitachi field emission scanning electron microscopy (SEM) (SEM S-4800, Hitachi Japan). The microscopic morphology and structure of the sample granules were observed. A sample spraying treatment was performed according to the previous method[16] with an accelerating voltage of 1.0 kV and an amplification factor of 1000 times.

2.7.2 FT-IR spectroscopy. The samples were analyzed using Fourier-transform infrared spectroscopy (FT-IR) spectra (IS50, Thermo Nicolet Corporation, America). The samples were mixed with dry KBr to obtain tablets that were determined in the range from 4000 to 400 cm^{-1}.

2.7.3 ^{1}H NMR spectra. The ^{1}H nuclear magnetic resonance (NMR) of samples was measured using an NMR spectrometer (BRUKER AVANCE III 400WB, Swiss, France) based on the previously described procedure.

2.8 Thermal performance analysis

Thermogravimetric analysis (TGA) was performed using a TGA Q600 (TA Instruments). Approximately, 5 mg of the samples were scanned from 25 to 700 °C at a heating rate of 10 °C min^{-1} under a nitrogen flow of 50 mL min^{-1}.

2.9 Antioxidant activity

The antioxidant activity measured using the 2,2-diphenyl-1-picrylhydrazyl (DPPH) radical scavenging reaction was evaluated by referring to the previously described procedure.[18] The absorbance was measured at 517 nm. The samples were stored at room temperature and were taken out at 1, 2, 3, 4, 5, 6, and 7 days for evaluation of the percentage of DPPH scavenging activity, respectively.

2.10 Statistical analyses

The SPSS statistical software version 21.0 (SPSS Inc., Chicago, IL, USA) was employed to analyze the significant differences among the means ($P < 0.05$) using Duncan's multiple range test.

3. Results and discussion

3.1 Characterization of the LR-CDs product

The MALDI-TOF mass spectrometry of the standard LR-CDs (CD_{22}–CD_{50}) and LR-CDs are shown in Fig. 1. The degree of polymerization of the LR-CDs mixture produced using rice starch was in the range of CD_9–CD_{22}, in which CD_9–CD_{15} were the main products (Fig. 1b) and the amount of CD_9–CD_{15} in the LR-CDs product was about 40 times higher than that obtained from the LR-CDs standard.[7] However, it was observed that the yield of the cyclodextrins with a size of over 22 was only a trace amount. As previously reported, raw tapioca starch can be used to obtain macrocyclodextrin with a degree of polymerization of CD_{21}–CD_{24} and CD_{37}–CD_{39}.[7] The discrepancy in the degree of CD polymerization and the yield in raw tapioca and rice starch was mainly caused by the difference in the amylose and amylopectin content. According to previous reports, the degree of polymerization and the yield of LR-CDs obtained are different depending on the type of enzyme, the substrate ingredients,[6] reaction temperature, and reaction time used.[19] It can be concluded that CGTase catalyzes the transglycosylation of rice starch to produce LR-CDs with the range of CD_9–CD_{22}.

It has been elucidated that LR-CDs were embedded as wall materials to improve the stability or solubility of the guest molecules.[6] CD_9–CD_{12} has a large hydrophobic inner cavity that is capable of forming a suitable inclusion complex with a guest molecule, which can be observed by the interaction of the δ-CD and Buckminsterfullerene (C_{70}).[5,20] The large cyclodextrin mixture with a polymerization degree of 20–50 interacted with guest molecules such as cholesterol and digitoxin. In this test, we tried to evaluate the process by which a mixture of LR-CDs (CD_9–CD_{22}) and tocopherol forms a substantial complex by co-precipitation.

3.2 Encapsulation efficiency results

The EE of different molar ratios of α-tocopherol/LR-CDs is shown in Fig. 2. The choice of guest molecule selected resulted from the fact that tocopherol was the most important natural antioxidant in vegetable oil and it has beneficial properties to protect these products from lipid peroxidation. The encapsulation of guest molecules by cyclodextrin requires a particular conditional process, and the co-precipitated form in aqueous solution was optimized for the complexation of α-tocopherol and macrocyclodextrin.

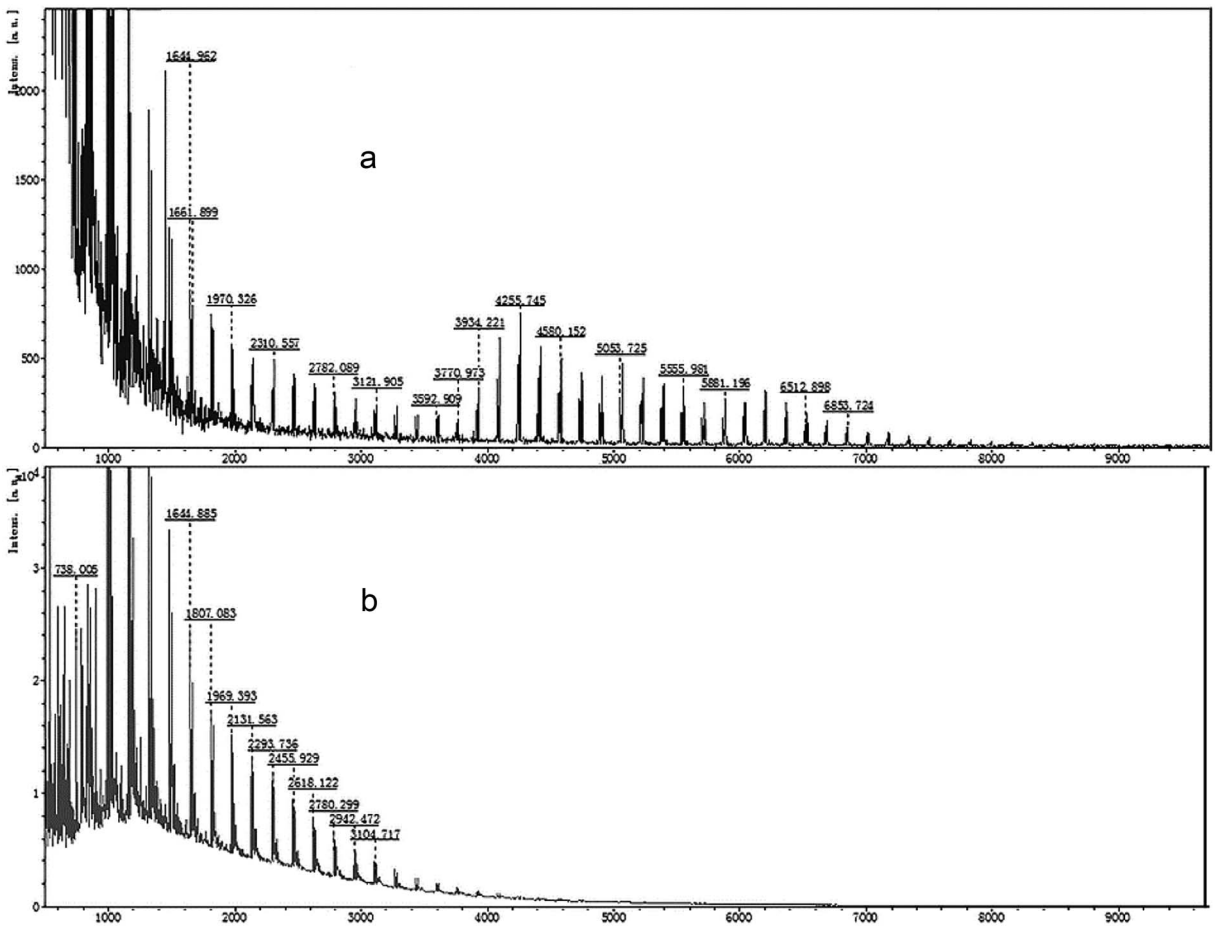

Fig. 1 MALDI-TOF mass spectrometry profiles of the LR-CDs: (a) a mixture of standard LR-CDs (CD_{22}–CD_{50}) and (b) the assignment of LR-CDs obtained from rice starch.

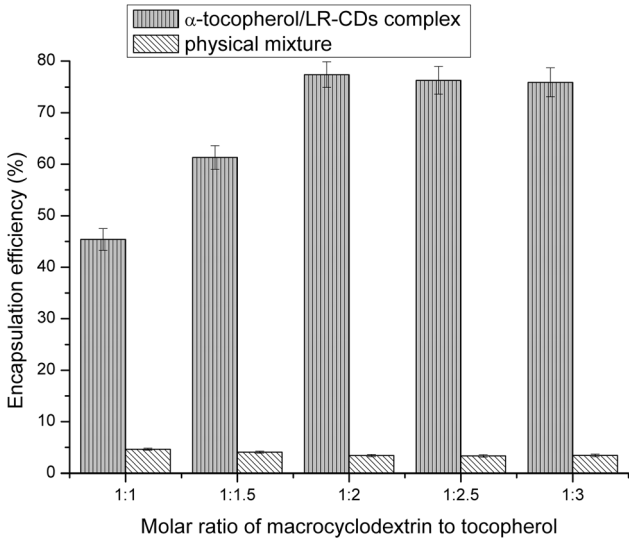

Fig. 2 The encapsulation efficiencies (%) of different molar ratios of α-tocopherol/LR-CDs.

The EE of the inclusion compound was between 42.8% and 76.4%. By changing the molar ratio of the LR-CDs to α-tocopherol, it was expressed as a percentage of the tocopherol content in the mixture and the initial content. It was found that α-tocopherol was captured in the cavity of the LR-CDs, and when the ratio increased from 1 : 1 to 1 : 2, more tocopherols were captured in the cavities of the LR-CDs, and when the ratio of α-tocopherol : LR-CDs was 1 : 2, the EE reached a maximum, and the tocopherol in the complex was found to be approximately 76%. However, as the ratio ranged from 1 : 2.5 to 1 : 3, a slow decrease in the EE was observed. This may be attributed to the interaction between the tocopherol and LR-CDs, as well as the chemical structure and the physico-chemical properties of the guest molecule.[21] We observed that the EE of the physical mixture was inadequate, and this may be due to the error in the adsorption of α-tocopherol in the sample. The ratio of the α-tocopherol/LR-CDs complex was chosen as 1 : 2 owing to the economic benefits of obtaining higher levels of the complex for further use.

3.3 Inclusion complex characterization

3.3.1 SEM. The surface morphologies of all of the samples can be seen in Fig. 3a–c, respectively. The LR-CDs may be a good wall material for the guest compound to form inclusion complexes.[6] The pure LR-CDs had an irregular flaky shape (Fig. 3c). In Fig. 3a, the physical mixtures revealed spherical particles mixed with fragments. After α-tocopherol was mixed with the LR-CDs, it was probable that α-tocopherol had adhered to the surface of the LR-CDs. The particle size and shape of the structure observed in the physical mixtures changed when compared to the inclusion complex. Fig. 3b showed the combination of spherical particles and mixed fragments form smaller clusters of particles which may indicate the formation of a complex.[22] Kringel[11] evaluated the morphology of β-CD and orange or eucalyptus essential oil inclusions which showed

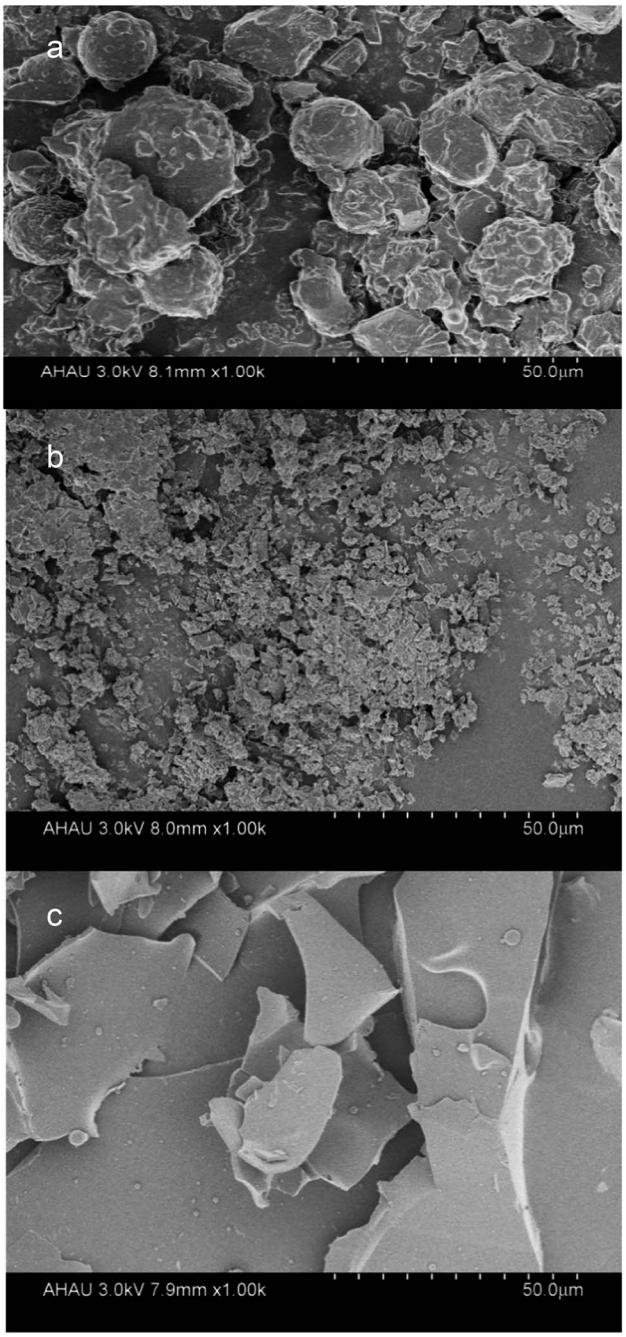

Fig. 3 Scanning electron micrographs of the LR-CDs–α-tocopherol physical mixture (a), the LR-CDs–α-tocopherol inclusion complex (b), and the LR-CDs (c). The magnification range of the samples was 1000×.

changes in the particle size and shape compared to pure β-CD. Thus, the morphologies of the inclusion complexes showed smaller clusters of particles, mainly because the LR-CDs were hydrophilic and have a V-shaped structure, which can exert a protective effect on the adhesion of tocopherols and can encapsulate α-tocopherols effectively.

3.3.2 FT-IR analysis. The FT-IR spectra of the inclusion complex, physical mixtures, α-tocopherol, and the LR-CDs are

shown in Fig. 4. No significant differences in the characteristic peak shape were found for the inclusion complex as compared to the free α-tocopherol at the main peak of 955 (O–H), 1158 (C–O), 1750 (C=O), 2857 (CH_3) and 2928 cm^{-1} $(CH_2)_n$. However, the signal intensity of these bands decreased. According to the previous reports, the embedding of the guest molecules decreased the movement and signal intensity of the encapsulated molecules.[23,24] Changes in the characteristic bands of the guest molecules, such as the decrease in the peak intensity, disappearance, and broadening, were attributed to the limitation of the tensile vibration of the guest molecules contained in the CD cavity, indicating that these bonds can participate in these complexes.[16] In addition, compared to the LR-CDs, there was no change in the OH-bending (1641 cm^{-1}) absorption bands, and the C–O–C bending of the glycosidic bond (1030 cm^{-1}). The obtained results indicate that the characteristic peaks of the LR-CDs and α-tocopherol were found in the complex. The decrease in the peak signal of the two components indicated the interaction between the molecules, but the degree of vibration of the frequency band was not changed.[7]

In addition, the characteristic absorption band of the physical mixture showed a combination of the individual spectra of the α-tocopherol and the LR-CDs, indicating that almost no interaction between the molecules occurred (Fig. 4). The FT-IR spectrum of α-tocopherol showed characteristic bands at 1750, 955, and 2928 cm^{-1} which were considered to be caused by the stretching of C=O, O–H, and C–H, respectively (see Table 1).[25] The FT-IR spectrum of the LR-CDs showed characteristic bands at 3308 and 1030 cm^{-1} which were considered to be caused by the stretching of the O–H and C–O–C, respectively. In addition, the inclusion complex was compared with the LR-CDs, and a shift in the OH stretch was changed from 3321 to 3308 cm^{-1}, which indicated that the hydrogen bonding between the LR-CDs and α-tocopherol also increased significantly.

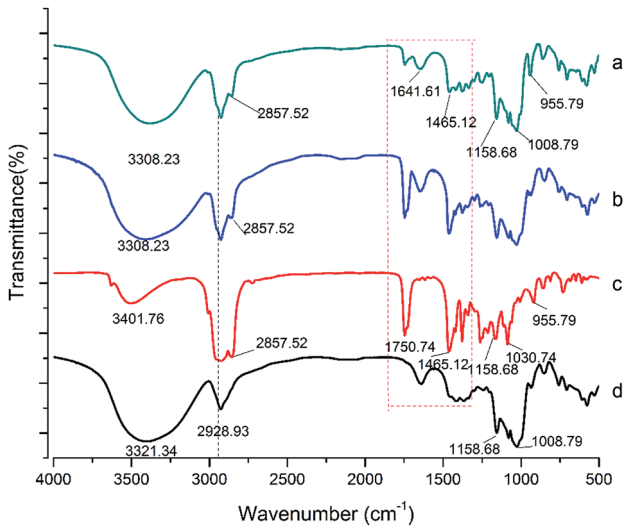

Fig. 4 FT-IR spectra of the LR-CDs–α-tocopherol inclusion complex (a), the LR-CDs–α-tocopherol physical mixture (b), α-tocopherol (c), and the LR-CDs (d).

3.3.3 NMR analysis. The ^{1}H NMR spectra of the LR-CDs, α-tocopherol, the inclusion complexes, and the physical mixture in DMSO-d_6 are shown in Fig. 5. ^{1}H NMR spectroscopy has been used to study and characterize the embedded tools to verify the true formation of the LR-CDs–α-tocopherol inclusion complexes.[26] In order to explore the inclusion complex, we compared the ^{1}H NMR spectra of the inclusion complex, the physical mixture, and the pure samples. A significant chemical shift existed for the O–H of the LR-CDs–α-tocopherol inclusion complexes. The ^{1}H NMR spectrum of the LR-CDs as an evaluation complex of the inclusion complex clearly demonstrated that the presence of the framework proton of the LR-CDs molecule shows a chemical shift of 0.3 ppm. These chemical shifts showed subtle changes as the interaction between them is a non-covalent bond. The signal for the LR-CDs in the formed complex was shifted compared to the signal for the physical mixing complex, while the signal for pure α-tocopherol was changed upon recombination. This observation suggested the possible inclusion mode of the complex as illustrated in the NMR spectra (Fig. 6). Combined with the results of the FT-IR and ^{1}H NMR analysis, it can be concluded that the LR-CDs–α-tocopherol inclusion complexes have been successfully prepared.

3.4 Thermogravimetric analysis

Fig. 6 presents the TGA of the LR-CDs, α-tocopherol, the inclusion complexes, and the physical mixture. This analysis showed the decomposition of LR-CDs in three zones. The initial weight loss occurred under 100 °C with an 8.8% mass loss in the first zone, which was related to the superficial water associated with the LR-CDs. The second stage occurred at around 105 °C with a 2.5% mass loss, which was related to the evaporation of internal water. However, a third process occurred at around 300 °C with a 73.5% mass loss that could be related to the degradation of the macrocycles.[11]

The complex formed by the interaction between macrocyclodextrin and tocopherol dramatically improved the thermal stability of tocopherol. The LR-CDs–α-tocopherol inclusion complex showed a higher thermal stability,[27] with a 83.1% mass loss and a temperature of decomposition of around 330 °C. In addition, the three stages of mass loss can also be observed from the TGA curve of the physical mixture. The mass loss in the first stage of the physical mixture was higher than that of the inclusion complex.[28] Meanwhile, the first zone at around 105 °C with a 45.4% mass loss was mainly due to the evaporation loss of the superficial water and α-tocopherol. Furthermore, the TGA curves of α-tocopherol indicated that the weight loss occurred at around 163.68 °C presented as 99.1% owing to the evaporation of the essential components[27]. Compared to the physical mixture and α-tocopherol, LR-CDs–α-tocopherol showed a slower weight loss rate and a reduced total weight loss, which indicated that the molecules have greater opportunities for entanglement and aggregation at higher temperatures.[18] It can be concluded that the inclusion complex can enhance the thermal stability and this suggests the formation of inclusion complexes.

Table 1 The main characteristic peaks for α-tocopherol, the LR-CDs and the LR-CDs–α-tocopherol complex.

Wavenumber (cm^{-1})		
α-Tocopherol	LR-CDs	LR-CDs–α-tocopherol
2857: CH_2	3308: O–H (stretching)	3308: O–H (stretching)
1750: C=O (stretching)	2928: CH_2 (stretching)	2857: CH_3
1158: C–O (stretching)	1641: O–H (bending)	1641: O–H (bending)
2928: CH_2 (stretching)	1158 and 1008: C–O and C–O (stretching)	2928: CH_2 (stretching)
955: O–H	1030: C–O–C	1030: C–O–C
		1158 and 1008: C–O and C–O (stretching)
		955: O–H

3.5 Antioxidant activity

2,2-Diphenyl-1-picrylhydrazyl is widely used to test the antioxidant activities of the different molecules for the scavenging of free radicals. The antioxidant activity is an essential characteristic of α-tocopherol. The DPPH scavenging activity assay for the LR-CDs–α-tocopherol complex, the physical mixture and the free form of the α-tocopherol can be seen in Fig. 7, respectively. It can be seen that the antioxidant activity of the LR-CDs–α-tocopherol complex is significantly higher than that of the physical mixture and the free form of α-tocopherol.[29] It can be observed that the physical mixture free radical scavenging ability was similar to that of the free α-tocopherol. We observed that three different forms of the antioxidant activity were decreased, but the α-tocopherol and the physical mixture were decreased more rapidly at ambient temperature (25 ± 1 °C) for seven days. This may be due to the presence of the phenolic hydroxyl groups in the molecule of α-tocopherol.[14] The DPPH scavenging ability of α-tocopherol decreased rapidly from 80.2% to 15.3%. Correspondingly, the complex decreased from 80.6% to 42.7%. This indicated that the LR-CDs–α-tocopherol inclusion complex could stabilize the antioxidant activity of α-tocopherol. This may be because LR-CDs were used as a wall material, which was a barrier to avoid the damage caused by temperature and oxygen, thereby improving the stability of the antioxidant. At the same time, it can be concluded that the embedded material retained the stability of α-tocopherol during storage. The LR-CDs–α-tocopherol complexes can improve the

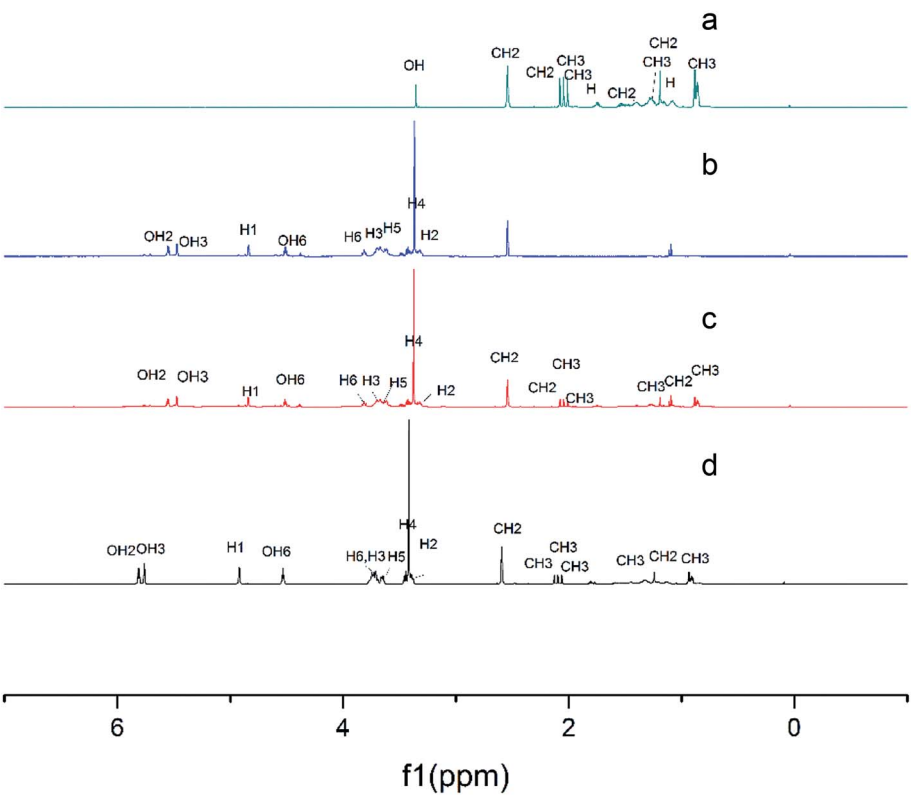

Fig. 5 ^{1}H NMR spectra of α-tocopherol (a), the LR-CDs (b), the physical mixture (c), and the inclusion complex (d).

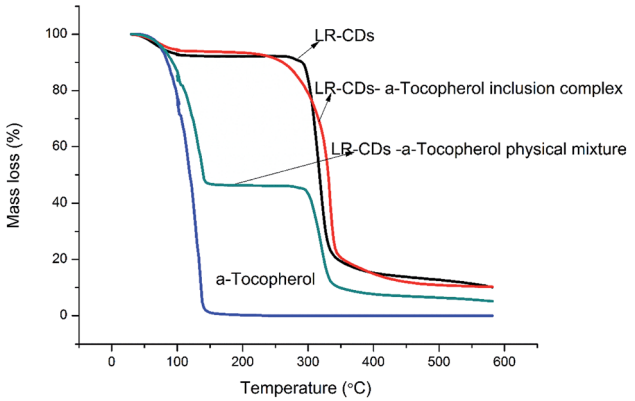

Fig. 6 TGA curves for the LR-CDs, α-tocopherol, the inclusion complex, and the physical mixture.

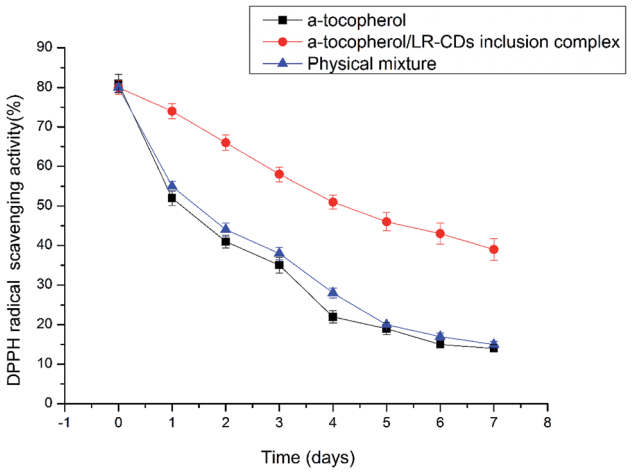

Fig. 7 The DPPH scavenging activity assay results for the LR-CDs–α-tocopherol complex, the physical mixture and the free form of α-tocopherol.

stability of α-tocopherol and expand their use in the food industry.

4. Conclusions

To summarize, our study suggested the potential for the synthesis of CGTase in rice starch, while LR-CDs (CD_9–CD_{22}) successfully encapsulated α-tocopherol. The complex prepared with a ratio of LR-CDs to α-tocopherol of 1 : 2 showed a high encapsulation efficiency. SEM images showed changes in the particle sizes and shapes of the observed structures relating to the LR-CDs–α-tocopherol inclusion complex, indicating the combination of spherical particles and mixed fragments. The formation of α-tocopherol/LR-CDs embedding was confirmed by X-ray diffraction (XRD), FT-IR, and ^{1}H NMR studies. At the same time, the LR-CDs–α-tocopherol inclusion complex could improve the thermal stability and antioxidant activity of α-tocopherol. Therefore, the use of LR-CDs in the formation of inclusion complexes showed high potential for being applied to embedding antioxidants in active food packaging.

Conflicts of interest

The authors declare no conflicts of interest.

Acknowledgements

This study was financially supported by a grant from the "Twelfth Five Year Plan for Science and Technology" of Anhui Province, China (No. 1401032009), and the Anhui Scientific and Technical Tackle-Key-Problem Plan (grant 1704a07020098).

References

1 Y. Terada, H. Sanbe, T. Takaha, S. Kitahata, K. Koizumi and S. Okada, *Appl. Environ. Microbiol.*, 2001, **67**, 1453–1460.
2 Y. Terada, M. Yanase, H. Takata, T. Takaha and S. Okada, *J. Biol. Chem.*, 1997, **272**, 15729–15733.
3 T. Endo, M. Y. Zheng and W. Zimmermann, *Aust. J. Chem.*, 2002, **55**(44), 39–48.
4 J. Jacob, K. Geßler, D. Hoffmann, H. Sanbe, K. Koizumi, S. M. Smith, T. Takaha and W. Saenger, *Angew. Chem., Int. Ed.*, 2010, **37**, 605–609.
5 K. L. Larsen, *Cheminform*, 2003, **43**, 1–13.
6 H. Ueda, *J. Inclusion Phenom.*, 2002, **44**, 53–56.
7 K. Kuttiyawong, S. Saehu, K. Ito and P. Pongsawasdi, *Process Biochem.*, 2015, **50**, 2168–2176.
8 Y. Sueishi, M. Hori and N. Inazumi, *J. Inclusion Phenom.*, 2012, **72**, 467–472.
9 C. C. Chen and G. Wagner, *Chem. Eng. Res. Des.*, 2004, **82**, 1432–1437.
10 F. Nacka, M. Cansell, P. Méléard and N. Combe, *Lipids*, 2001, **36**, 1313.
11 D. H. Kringel, M. D. Antunes, B. Klein, R. L. Crizel, R. Wagner, R. P. de Oliveira, A. R. G. Dias and E. da R. Zavareze, *J. Food Sci.*, 2017, **82**, 2598–2605.
12 G. Liu, Y. Hong, Z. Gu, Z. Li and L. Cheng, *Food Hydrocolloids*, 2015, **45**, 351–360.
13 T. Vongpichayapaiboon, P. Pongsawasdi and K. Krusong, *J. Appl. Microbiol.*, 2016, **120**, 912–920.
14 J. L. Koontz, J. E. Marcy, S. F. O'keefe and S. E. Duncan, *J. Agric. Food Chem.*, 2009, **57**, 1162–1171.
15 P. J. Fei, Q. C. Xiao, Z. Y. Hong and Y. Ling, *J. Food Process. Preserv.*, 2010, **34**, 114–124.
16 C. Cao, M. Shen, J. Hu, J. Qi, P. Xie and Y. Zhou, *CyTA–J. Food*, 2020, **18**(1), 84–93.
17 L. E. Hill, C. Gomes and T. M. Taylor, *LWT–Food Sci. Technol.*, 2013, **51**, 86–93.
18 X. Cai, X. Du, D. Cui, X. Wang, Z. Yang and G. Zhu, *Food Hydrocolloids*, 2019, **91**, 238–245.
19 Q. Qi, X. She, T. Endo and W. Zimmermann, *Tetrahedron*, 2004, **60**, 799–806.
20 K. Tomono, A. Mugishima, T. Suzuki, H. Goto, H. Ueda, T. Nagai and J. Watanabe, *J. Inclusion Phenom. Macrocyclic Chem.*, 2002, **44**, 267–270.
21 L. M. M. Gomes, N. Petito, V. G. Costa, D. Q. Falcão and K. G. D. L. Araújo, *Food Chem.*, 2014, **148C**, 428–436.

22 L. Wang, S. Li, P. Tang, J. Yan, K. Xu and H. Li, *Carbohydr. Polym.*, 2015, **129**, 9–16.
23 V. E. de Oliveira, E. W. C. Almeida, H. V Castro, H. G. M. Edwards, H. F. Dos Santos and L. F. C. de Oliveira, *J. Phys. Chem. A*, 2011, **115**, 8511–8519.
24 J. G. Galvão, V. F. Silva, S. G. Ferreira, F. R. M. França, D. A. Santos, L. S. Freitas, P. B. Alves, A. A. S. Araújo, S. C. H. Cavalcanti and R. S. Nunes, *Thermochim. Acta*, 2015, **608**, 14–19.
25 L. Lin, Y. Zhu and H. Cui, *Lwt*, 2018, **97**, 711–718.
26 G. Delogu, C. C. A. Juliano and M. Usai, *Nat. Prod. Res.*, 2016, **30**, 2049–2057.
27 R. L. Abarca, F. J. Rodríguez, A. Guarda, M. J. Galotto and J. E. Bruna, *Food Chem.*, 2016, **196**, 968–975.
28 X. Zhu and W. Ping, *Spectrochim. Acta, Part A*, 2014, **132**, 38–43.
29 T. Kulisic, A. Radonic, V. Katalinic and M. Milos, *Food Chem.*, 2004, **85**, 633–640.